AMERICAN SOCIETY FOR MICROBIOLOGY | Infection and Immunity

FAD-I, a *Fusobacterium nucleatum* Cell Wall-Associated Diacylated Lipoprotein That Mediates Human Beta Defensin 2 Induction through Toll-Like Receptor-1/2 (TLR-1/2) and TLR-2/6

Sanghamitra Bhattacharyya,[a*] Santosh K. Ghosh,[a] Bhumika Shokeen,[b] Betty Eapan,[a] Renate Lux,[b] Janna Kiselar,[c] Stanley Nithianantham,[a*] Andrew Young,[d] Pushpa Pandiyan,[a] Thomas S. McCormick,[a,d] Aaron Weinberg[a]

Department of Biological Science, Case School of Dental Medicine, Cleveland, Ohio, USA[a]; School of Dentistry, University of California—Los Angeles, Los Angeles, California, USA[b]; Center for Proteomics, Case School of Medicine, Cleveland, Ohio, USA[c]; Department of Dermatology, Case School of Medicine, Cleveland, Ohio, USA[d]

We previously identified a cell wall-associated protein from *Fusobacterium nucleatum*, a Gram-negative bacterium of the oral cavity, that induces human beta defensin 2 (hBD-2) in primary human oral epithelial cells (HOECs) and designated it FAD-I (*Fusobacterium*-associated defensin inducer). Here, we report differential induction of hBD-2 by different strains of *F. nucleatum*; ATCC 25586 and ATCC 23726 induce significantly more hBD-2 mRNA than ATCC 10953. Heterologous expression of plasmid-borne *fadI* from the highly hBD-2-inducing strains in a Δ*fadI* mutant of ATCC 10953 resulted in hBD-2 induction to levels comparable to those of the highly inducing strains, indicating that FAD-I is the principal *F. nucleatum* agent for hBD-2 induction in HOECs. Moreover, anti-FAD-I antibodies blocked *F. nucleatum* induction of hBD-2 by more than 80%. Recombinant FAD-I (rFAD-I) expressed in *Escherichia coli* triggered levels of hBD-2 transcription and peptide release in HOECs similar to those of native FAD-I (nFAD-I) isolated from *F. nucleatum* ATCC 25586. Tandem mass spectrometry revealed a diacylglycerol modification at the cysteine residue in position 16 for both nFAD-I and rFAD-I. Cysteine-to-alanine substitution abrogated FAD-I's ability to induce hBD-2. Finally, FAD-I activation of hBD-2 expression was mediated via both Toll-like receptor-1/2 (TLR-1/2) and TLR-2/6 heterodimerization. Microbial molecules like FAD-I may be utilized in novel therapeutic ways to bolster the host innate immune response at mucosal surfaces.

The epithelial surfaces of the oral cavity are sites of active bacterial colonization. While colonizing, certain bacteria promote activation of human beta defensin (hBD) expression in the oral mucosa (1–3). By virtue of their antimicrobial and immunoregulatory properties, these epithelial-cell-derived innate response peptides contribute to the homeostasis between the bacterium and the host (4). Human beta defensin 2 (hBD-2) and hBD-3 are the two inducible members of the hBD peptide family that we and others have described in the oral cavity (1, 5–10). Interestingly, while hBD-3 is associated with the highly proliferating, nondifferentiated stratum basale of the oral mucosa, hBD-2 is compartmentalized in the more superficial stratum spinosum and stratum granulosum; i.e., nonproliferating yet differentiating regions of the oral mucosa (11, 12). This, along with other results showing that hBD-2 is induced as a result of inflammation via MAPK or NFκB (5) while hBD-3 is activated through epidermal growth factor receptor (13, 14), strongly suggests that the latter is more involved in wound healing while the former plays a more active role in inhibiting microbial invasion during mucosal-barrier disruption (15–17). Moreover, in addition to their antimicrobial properties (18, 19), both peptides have been shown to act as chemokines in recruiting lymphoid and myeloid cells from the bloodstream (20).

Fusobacterium nucleatum, a ubiquitous Gram-negative bacterium of the human oral cavity, has been extensively studied for its properties of adhesion to other bacteria, an important feature in oral biofilm formation (21, 22). In addition to its role in oral community architecture, we and others have shown that the cell wall of *F. nucleatum* induces hBD-2 expression in normal primary human oral epithelial cells (HOECs) (1, 5, 10, 23). The presence of *F. nucleatum* in oral biofilms colonizing oral surfaces may be a reason why the generally inducible hBD-2 is constitutively expressed in the upper strata of the oral mucosa, a trait apparently unique to this site compared to other mucosal body sites (5, 11, 17). We have also shown that, as well as in HOECs, *F. nucleatum* is also capable of inducing hBD-2 in skin keratinocytes (14).

Recently, we reported the identification, isolation, and functional evaluation of a cell wall-associated protein from *F. nucleatum* that induces hBD-2 in HOECs (1). We named this protein *Fusobacterium*-associated defensin inducer (FAD-I). Expression of FAD-I in a bacterium (*Porphyromonas gingivalis* ATCC 33277) that did not promote hBD-2 expression resulted in its ability to do so (1). Here, we present new evidence showing that (i) FAD-I is the principal *F. nucleatum* molecule responsible for hBD-2 induc-

Received 19 October 2015 **Returned for modification** 20 November 2015
Accepted 13 February 2016

Accepted manuscript posted online 29 February 2016

Citation Bhattacharyya S, Ghosh SK, Shokeen B, Eapan B, Lux R, Kiselar J, Nithianantham S, Young A, Pandiyan P, McCormick TS, Weinberg A. 2016. FAD-I, a *Fusobacterium nucleatum* cell wall-associated diacylated lipoprotein that mediates human beta defensin 2 induction through Toll-like receptor-1/2 (TLR-1/2) and TLR-2/6. Infect Immun 84:1446–1456. doi:10.1128/IAI.01311-15.

Editor: S. M. Payne

Address correspondence to Aaron Weinberg, aaron.weinberg@case.edu.

* Present address: Sanghamitra Bhattacharyya, Department of Pathology, Case School of Medicine, Cleveland, Ohio, USA; Stanley Nithianantham, Department of Molecular and Cellular Biology, University of California, Davis, California, USA.

Supplemental material for this article may be found at http://dx.doi.org/10.1128/IAI.01311-15.

tion; (ii) FAD-I is posttranslationally modified at its cysteine in position 16 (C16) by a diacylglycerol, which is essential for FAD-I-dependent hBD-2 activation in HOECs; and (iii) FAD-I induces hBD-2 in HOECs through both Toll-like receptor-1/2 (TLR-1/2) and TLR-2/6. Since most mucosal body sites do not express constitutive levels of hBD-2, FAD-I, or its derivatives, offers the possibility of inducing the body's own innate antimicrobial agents in vulnerable mucosa.

MATERIALS AND METHODS

HOEC culture and treatment. Tissue acquisition for primary cell isolation was conducted in accordance with our Institutional Review Board (IRB)-approved protocol (NHR-15-19) for the use of discarded tissue. Primary HOECs were expanded from tissues overlying impacted third molars, as previously described (24), and grown as monolayers to ~70% confluence. The cells were cultured in EpiLife medium (Gibco, Life Technologies) supplemented with 1% penicillin-streptomycin, 0.2% Fungizone, and 1% human keratinocyte growth supplement (HKGS) (Gibco) at 37°C and 5% CO_2 prior to challenge with various agents.

HOECs that reached ~70% confluence were trypsinized, split, and seeded in 12- or 24-well plates at concentrations of 1.7×10^5 and 3.5×10^5 cells/well, respectively. The plates were incubated for 1 or 2 days until the cells reached ~80% confluence. These cells were then used for the various experiments described below. Incubations with the various agents were for ~18 h.

Construction of *F. nucleatum* mutant and complementation strains. For generation of an *F. nucleatum* ATCC 10953 mutant derivative lacking FAD-I, allelic-exchange mutagenesis was used to replace the ATCC 10953 *fadI* gene with the *catP* gene resistance cassette. Briefly, the construct was generated by fusing 1 kb of DNA upstream and downstream of *fadI* with the *catP* gene, along with its promoter. The upstream region was amplified from *F. nucleatum* ATCC 10953 using primer pair BS933/BS934, while the downstream region was amplified using the primer pair BS937/BS938. The *catP* gene was PCR amplified from pHS30 (25) using primers BS935 and BS936. The primers contained an overlap of 25 to 30 bp to allow fusion in PCRs, and the fusion PCR was carried out as described by Shevchuk et al. (26). The fusion product was cloned into pCR-BluntII-TOPO (Invitrogen) and confirmed by sequencing. The plasmid DNA was electroporated into *F. nucleatum* ATCC 10953 as described by Haake et al. (25) and plated on selective medium containing thiamphenicol to obtain the corresponding Δ*fadI* derivative. The genomic DNA of the obtained colonies was analyzed by PCR for the presence of the *catP* gene and the absence of *fadI*. One of the colonies was designated the Δ*fadI* inactivated mutant for complementation with heterologous expressed *fadI* from highly hBD-2-inducing *F. nucleatum* strains ATCC 23726 and ATCC 25586 under the control of the *fomA* promoter. The *fadI* genes of *F. nucleatum* ATCC 23726 and ATCC 25586 were amplified from the respective genomes using the primer pair BS926/BS927. The *fomA* promoter was amplified from *F. nucleatum* 10953 using the primer pair BS924/BS925. The fused products of the *fomA* promoter and the respective *fadI* genes were cloned into the shuttle vector pHS58 (27). All the resulting plasmids were confirmed by sequencing and transformed into the Δ*fadI* derivative of *F. nucleatum* ATCC 10953 for complementation and heterologous expression of the different *fadI* genes. The presence of the fusion construct between the *fomA* promoter and *fadI* from ATCC 25586 and ATCC 23726 in the transformants was confirmed by PCR. The primer pairs used are described in Table S1 in the supplemental material.

Isolation of FnCW. *F. nucleatum* cell wall (FnCW) extracts from different *F. nucleatum* parent and mutant strains were prepared as previously described (28).

Isolation of nFAD-I. Native FAD-I (nFAD-I) was isolated from FnCW extracts derived from *F. nucleatum* ATCC 25586 by immunoprecipitation using a polyclonal anti-FAD-I antibody (1). To eliminate nonspecific interactions, 100 μg of the bacterial cell wall fraction was initially incubated with 50 μl of preimmune serum at 4°C overnight in the presence of antibody binding buffer (Thermo Scientific, Waltham, MA) and protease inhibitors (Thermo Scientific). Precleared lysates were obtained by adding 25 μl of protein A magnetic beads (Novex, Life Technologies) to the mixture. Thirty micrograms of the anti-FAD-I antibody was added to the supernatants and continuously mixed at 4°C overnight. The magnetic beads were washed with antigen-antibody binding buffer (Thermo Scientific). nFAD-I was eluted out of the complex at room temperature with Gentle antigen elution buffer (Thermo Scientific) by 40 min of incubation at room temperature with constant rotation. The isolated protein was further dialyzed against Tris buffer (pH 7.5) at 4°C overnight, and the protein content was measured with a Dc protein assay kit (Bio-Rad, Hercules, CA). The protein was identified by mass spectrometric (MS) analysis (Proteomics Core, Case Western Reserve University [CWRU]).

Cloning and bacterial overexpression of rFAD-I. The full-length FAD-I gene (FN1527) (1) was amplified by PCR from genomic DNA of *F. nucleatum* strain ATCC 25586 using primers (see Table S2 in the supplemental material) with Nde1 and Xho1 restriction sites at their ends (New England BioLabs). The PCR product was gel purified using a PCR purification kit (Qiagen, Germantown, MD) and cloned in the pET-20b vector (Novagen). Recombinant FAD-I (rFAD-I) protein was overexpressed from one positive clone in the host *Escherichia coli* BL21(DE3) (Invitrogen, Life technologies). The *E. coli* culture, maintained at 37°C with 1 mM IPTG (isopropyl-β-D-thiogalactopyranoside), generated the recombinant protein within 4 h. Bacterial cells were harvested by centrifugation at 4,000 rpm for 10 min, and the cell pellet was washed with 1× phosphate-buffered saline (PBS) and stored at −80°C until further processed. Different mutant forms of FAD-I (Δ15, C16A, and 15-amino-acid signal sequence) (see Fig. S1 in the supplemental material) were generated using a Quick Site-Directed Mutagenesis kit (Stratagene, La Jolla, CA) with the full-length FAD-I gene of *F. nucleatum* strain ATCC 25586 as the template. The primers used for creating the mutants are listed in Table S2 in the supplemental material. Cloning and overexpression were conducted in pET20b following the same protocol used to generate the full-length FAD-I protein.

Purification of overexpressed proteins from *E. coli*. *E. coli* cell pellets overexpressing complete FAD-I, the Δ15 and C16A derivatives, or the signal peptide (SP) were suspended in 50 mM Na_2HPO_4, 100 mM NaCl (pH 7.5), 0.1 mM phenylmethylsulfonyl fluoride (PMSF), and 1× Halt protease inhibitor (Thermo Scientific) and sonicated on ice using a Fisher Sonic Dismembrator 300 (Thermo Fisher, Bridgewater, NJ) on ice. The cells were subjected to 20 cycles of 5-s pulses repeated 5 times with a wait time of 2 to 3 min after each cycle. The lysed cells were centrifuged at 18,000 rpm and 4°C for 30 min. The supernatant underwent further processing to isolate the desired protein using a Qiaexpress Ni-nitrilotriacetic acid (NTA) column (Qiagen), following the manufacturer's protocol. The His-tagged column eluent was dialyzed against 10 mM Tris-HCl, pH 7.5, and 100 mM NaCl. The dialyzed protein was concentrated using an Amicon tube concentrator with a 5-kDa cutoff (Millipore, MA). The recombinant signal sequence was expressed in inclusion bodies. Recovery of the overexpressed protein from the inclusion bodies and its purification were done using inclusion body solubilization reagent (Thermo Scientific) according to the manufacturer's protocol.

Mass spectrometric analysis. A C_{18} reverse-phase column was utilized for identification of possible posttranslational modifications (PTM), including phosphorylation, myristoylation, and sulfonation. Approximately 300 ng of both the rFAD-I and the nFAD-I peptide mixtures was loaded onto a 100-μm by 2-cm Acclaim PepMap100 C_{18} reverse-phase trapping column to preconcentrate and wash away excess salts using a nano-UltiMate-3000 Rapid Separation LC system (Dionex, Sunnyvale, CA). The reverse-phase separation was performed on a 75-μm by 25-cm (particle size, 2 μm, and pore size, 100 A) Acclaim PepMap100 C_{18} reverse-phase column (Dionex) using a linear gradient of 5 to 60% buffer B (100% acetonitrile-0.1% formic acid [FA]) over 55 min.

A C_4 reverse-phase column was utilized for identification of lipid modification only. The approximately 300 ng of digest mixture derived

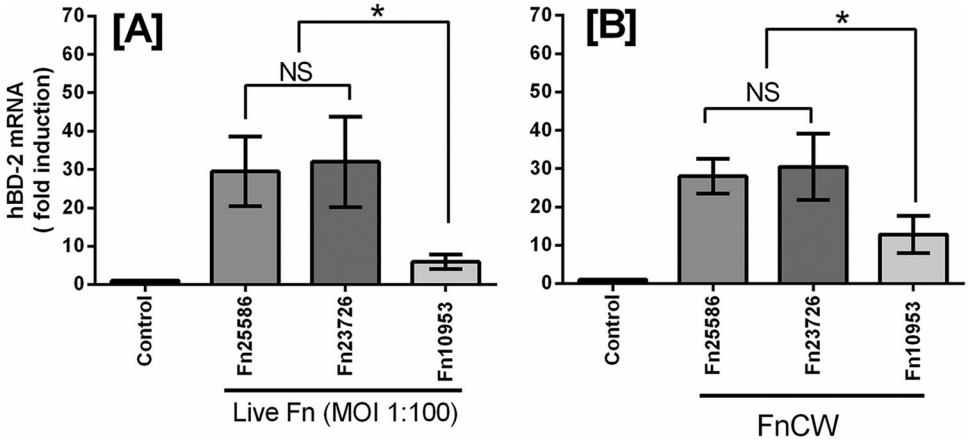

FIG 1 Induction of hBD-2 mRNA by live bacterial cells (A) and cell wall preparations (10 μg/ml cell wall *F. nucleatum* [Fn] ATCC 25586, ATCC 23726, and ATCC 10953 (B). The data presented are means ± standard deviations (SD) of the results of three to six replicate experiments; *, significant ($P < 0.05$), and NS, not significant between the indicated experiments.

from both the rFAD-I and the nFAD-I proteins was loaded onto a 100-μm by 2-cm Acclaim PepMap100 C_{18} reverse-phase trapping column to preconcentrate and wash away excess salts using a nano-UltiMate-3000 Rapid Separation LC system (Dionex, Sunnyvale, CA). The reverse-phase separation was performed on a 75-μm by 15-cm (particle size, 5 μm, and pore size, 300 A) Acclaim PepMap300 C_4 reverse-phase column (Dionex) using a linear gradient of 20 to 100% buffer B over 64 min.

Proteolytic peptides eluting from either C_{18} or C_4 columns were directed to an LTQ-FT mass spectrometer (Thermo Fisher Scientific, Wilmington, DE) equipped with a nanospray ion source with a needle voltage of 2.4 kV. All mass spectra were obtained from data-dependent experiments in the positive ion mode. MS and tandem-MS (MS-MS) spectra were acquired with full-scan MS recorded in the FT analyzer at a resolution (*R*) of 100,000, followed by MS-MS of the eight most intense peptide ions in the LTQ analyzer. The data were analyzed by searching tandem-MS spectra using Mascot software against a database containing FN1527 protein, considering variable modification of S, T, and Y residues by 79.966 Da; S, T, and Y residues by 79.957 Da; C residues by 210.198 Da; and C residues by 576.511 Da, which correspond to phosphorylation, sulfation, myristoylation, and *S*-diacylglycerol cysteine, respectively.

RNA isolation, quantitative PCR (qPCR), and enzyme-linked immunosorbent assay (ELISA). RNA was extracted from HOECs with the RNeasy minikit (Qiagen) following the manufacturer's instructions. The RNA concentration was measured by UV absorbance at 260/280 nm using a Nanodrop 1000 (Thermo Fisher Scientific). Quantitative real-time PCR was performed with a Bio-Rad CFX96 system with a high-capacity cDNA reverse-transcription kit (Applied Biosystems, Carlsbad, CA) and SyBr Green Supermix (Bio-Rad) according to the manufacturer's protocol. The primer sequences for hBD-2 and the glyceraldehyde-3-phosphate dehydrogenase (GAPDH) housekeeping gene are shown in Table S2 in the supplemental material. Primers were designed using Primer3 primer design software (29) and were analyzed using Oligo Analysis (Integrated DNA Technologies [IDT]) in order to avoid secondary structures. The medium supernatants from HOECs were analyzed for hBD-2 protein levels following our previously described protocol (9, 10).

Flow cytometry. Biotin-conjugated anti-TLR-1, allophycocyanin (APC)-conjugated anti-TLR-2, and phycoerythrin (PE)-conjugated anti-TLR-6 antibodies were used for flow cytometry (Ebiosciences, San Diego, CA). For surface staining, the cells were first harvested in cell dissociation buffer and then washed and stained in PBS- bovine serum albumin (BSA) (0.5%)-EDTA (0.5 mM) buffer for 1 h and immediately analyzed (LSR II Fortessa; BD Biosciences, CA). Cells were harvested in trypsin-EDTA and washed in PBS-BSA (0.5%)-EDTA (0.5 mM) buffer to remove surface proteins. Unconjugated antibodies were used to further block the remaining surface proteins. The cells were then fixed using 1× fixation buffer (Ebiosciences) overnight, followed by permeabilization and staining, using the conjugated antibodies mentioned above, in 1× permeabilization buffer (Ebiosciences) for 2 h, and analyzed by flow cytometry. Surface detection of the same receptor proteins was done with and without cytochalasin D (CytD) (Life Technologies) treatment. HOECs were pretreated with 40 μM cytochalasin D at 37°C 1 h prior to FAD-I stimulation. We also used fluorescein isothiocyanate (FITC)-labeled FAD-I (Bio Basic Canada Inc., Markham, Ontario, Canada) to measure the receptor-ligand association at the surface, as detected by TLR-2 and FAD-I–FITC-double-positive cells by flow cytometry.

Statistical analysis. All statistical analyses (Student *t* test or analysis of variance [ANOVA]) were performed using Graph Pad (La Jolla, CA) Prism v.6 software. *P* values of <0.05 were considered statistically significant.

RESULTS

FAD-I is the main inducer of hBD-2 in *F. nucleatum*. We have shown that *F. nucleatum* ATCC 25586 induces hBD-2 upon contact with primary HOECs (5). We screened two additional sequenced *F. nucleatum* strains (ATCC 23726 and ATCC 10953) for the ability to induce hBD-2 transcription by challenging HOECs with live bacterial cultures (multiplicity of infection [MOI], 1:100) and discovered that while hBD-2 mRNA induction by ATCC 23726 was similar to that by ATCC 25586, ATCC 10953 showed significantly less activity (Fig. 1A). We isolated FnCW fractions from each of the three strains and found that the fractions behaved like whole bacterial cells (Fig. 1B). To compare the levels of FAD-I protein in the whole-cell lysates of ATCC 10953 (a low inducer) with those of high-inducer strains (ATCC 25586 and ATCC 23726), we performed Western immunoblot analysis, which revealed relatively low levels of FAD-I in ATCC 10953 compared to those in high-inducer strains (Fig. 2A; see Fig. S3 in the supplemental material). Additionally, alignment of the corresponding FAD-I sequences revealed that the proteins of strains ATCC 25586 and ATCC 23726 differed in only a single amino acid (99.2% similarity), while strain ATCC 10953 shared only 87.6% sequence similarity with either of the other two strains (Fig. 2B). Interestingly, the sequence differences between ATCC 10953 and the other two strains were found principally in the signal peptide

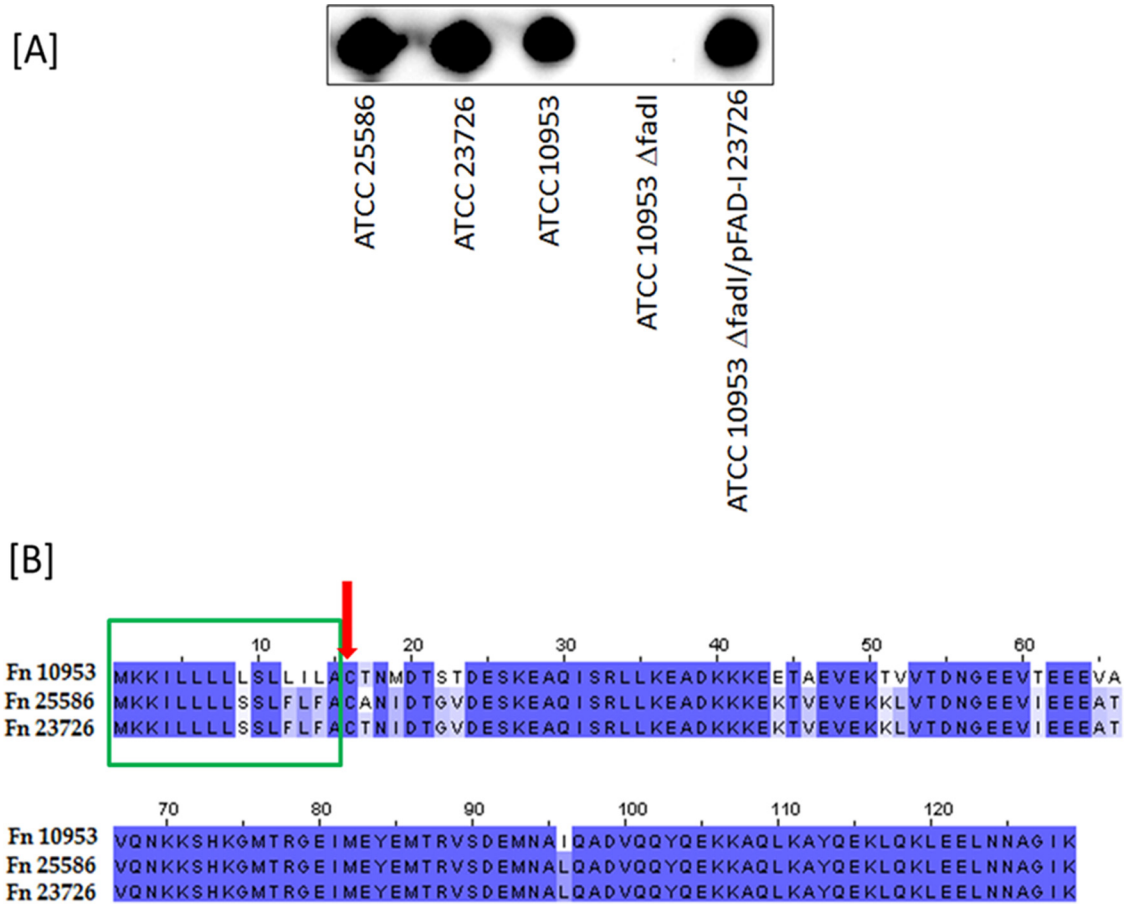

FIG 2 (A) Western immunoblot of FAD-I protein in whole-cell lysates of *F. nucleatum* ATCC 25586, ATCC 23726, ATCC 10953, ATCC 10953 Δ*fadI*, and ATCC 10953 Δ*fadI*/pFAD-I 23726 (ATCC 10953 Δ*fadI* with plasmid-based expression of FAD-I from ATCC 23726). For Western blotting, whole-cell lysates derived from 1.5×10^7 cells of the different *Fusobacterium* strains at the mid-logarithmic growth phase were resolved in a 4 to 12% SDS-PAGE precast gel (NuPAGE, Invitrogen, USA) according to standard protocols, and anti-FAD-I antibody (1) was used to detect FAD-I. (B) Multiple-sequence alignment of FAD-I peptides from three *F. nucleatum* strains (ATCC 25586, ATCC 23726, and ATCC 10953). The Clustal W (54) Web-based service was used to align the sequences. The arrow indicates a conserved cysteine; the box at the N terminus indicates the signal peptide sequences; the dark-blue-shaded amino acids are common to all three proteins, while the amino acids shaded light blue or white indicate differences in sequences.

region of FAD-I, along with various sites in the mature-peptide region (Fig. 2B).

Since *F. nucleatum* ATCC 10953 has a greatly reduced ability to trigger hBD-2 transcription in HOECs, it provides an ideal background to test whether FAD-I is the key agent produced by *F. nucleatum* for induction of hBD-2. To remove possible FAD-I background activity, we first created a mutant derivative of ATCC 10953 lacking the FAD-I-encoding gene (see Materials and Methods for details). The *fadI* genes of the highly hBD-2-inducing strains ATCC 25586 and ATCC 23726 were cloned into a fusobacterial shuttle vector under the control of a constitutive fusobacterial promoter and transformed into the ATCC 10953 Δ*fadI* mutant strain. The FAD-I production of the resulting strains was confirmed, and then the strains were tested for the ability to induce hBD-2 transcription in HOECs. Both ATCC 10953 Δ*fadI* derivatives expressing heterologous FAD-I of ATCC 25586 or ATCC 23726 displayed FAD-I activities similar to the respective highly hBD-2-inducing parent strains (Fig. 3A). The Western immunoblot for FAD-I expression in cell lysates of ATCC 10953 Δ*fadI* complemented with FAD-I of ATCC 23726 (a high inducer) showed a level of expression of FAD-I in cell lysates comparable to that of the parent highly inducing strain (Fig. 2A). Finally, addition of anti-FAD-I antibodies reduced hBD-2 induction by *F. nucleatum* ATCC 25586 cell wall fractions by more than 80% (Fig. 3C).

Recombinant FAD-I is as potent as native FAD-I in inducing hBD-2. We previously reported that FAD-I from *F. nucleatum* ATCC 25586 could be recombinantly expressed in *E. coli* (rFAD-I) and that the purified protein induces hBD-2 production (1). We now wanted to compare the hBD-2-inducing ability of rFAD-I with that of nFAD-I and purified both proteins (as described in Materials and Methods). Challenge of HOECs with either rFAD-I or nFAD-I resulted in comparable hBD-2 transcript expression and peptide release (see Fig. S1 in the supplemental material), and hence, we continued using rFAD-I in our subsequent studies due to easier manipulation and purification of the protein.

The signal peptide is important for FAD-I activity. Sequence analysis of FAD-I revealed that the full-length protein is comprised of 129 amino acids (14 kDa), with residues 1 to 15 (MKKI LLLLSSLFLFA) corresponding to the predicted signal sequence (Fig. 2; see Fig. S2 in the supplemental material). The processed mature protein, without the signal sequence, consists of 114 resi-

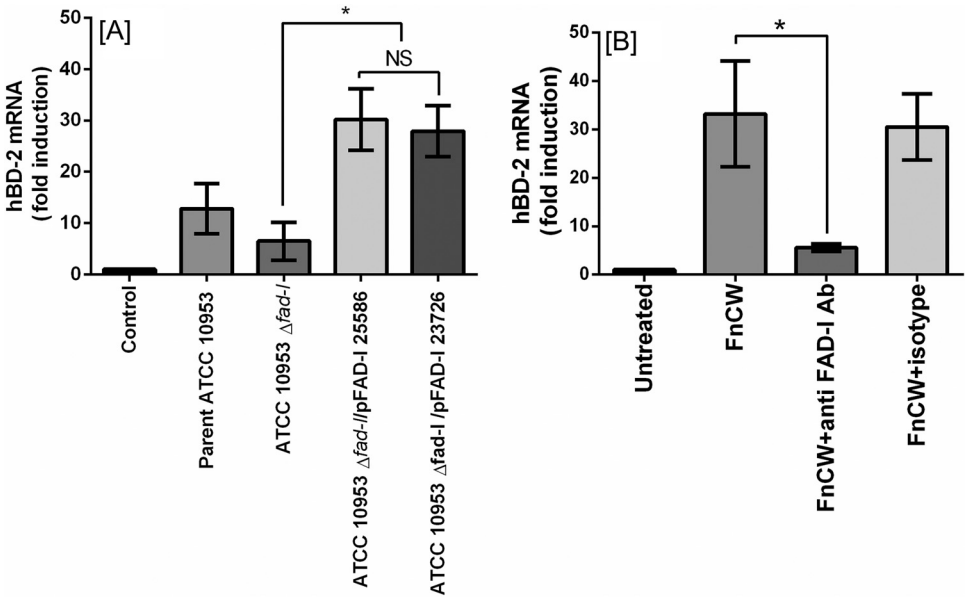

FIG 3 Induction of hBD-2 mRNA by cell wall preparations (10 μg/ml) of parent ATCC 10953, ATCC 10953 Δ*fadI*, ATCC 10953 Δ*fadI*/pFAD-I25586 (ATCC 10953 Δ*fadI* with plasmid-based expression of FAD-I from ATCC 25586), and ATCC 10953 Δ*fadI*/pFAD-I23726 (ATCC 10953 Δ*fadI* with plasmid-based expression of FAD-I from ATCC 23726) (A) and 25586 FnCW (10 μg/ml) (B) in the presence of anti-FAD-I antibody (1) or isotype control. The data presented are means ± SD of the results of three to six replicate experiments; *, significant ($P < 0.05$), and NS, not significant between the indicated treatments.

dues and is referred to as Δ15 FAD-I. We recombinantly produced mature FAD-I (Δ15 FAD-I) and SP as separate entities and compared their abilities to induce hBD-2 with that of full-length rFAD-I. Our results show that rFAD-I is significantly compromised upon deletion of the signal peptide (Fig. 4A and B). Interestingly, HOECs stimulated with the signal peptide alone and the signal peptide in conjunction with mature FAD-I (Δ15 FAD-I) were unable to induce hBD-2, indicating that the intact rFAD-I, containing its signal peptide, is essential for activity.

FAD-I is posttranslationally modified at the cysteine in position 16. The cysteine in position 16 is conserved (Fig. 2) in the predicted amino acid sequences of FAD-I proteins present in the three *F. nucleatum* strains tested. Further analysis of the FAD-I sequences of ATCC 25586, ATCC 23726, and ATCC 10953 with the ScanProsite tool (30) revealed a potential posttranslational lipid modification at C16 by either *S*-diacyl-glycerol or *N*-palmitoyl-cysteine (see Fig. S2 in the supplemental material). To confirm this modification and further analyze its nature, rFAD-I (Fig. 5A) and nFAD-I (Fig. 5B) proteins corresponding to *F. nucleatum* ATCC 25586 were digested with trypsin and analyzed by liquid chromatography (LC)–MS-MS (as described in Materials and Methods). A doubly protonated ion signal at *m/z* 914.53 that corresponds to the CANIDTGVDESK peptide (C16-K27) with a mass shift of 576.14 Da was observed. MS-MS analysis of doubly

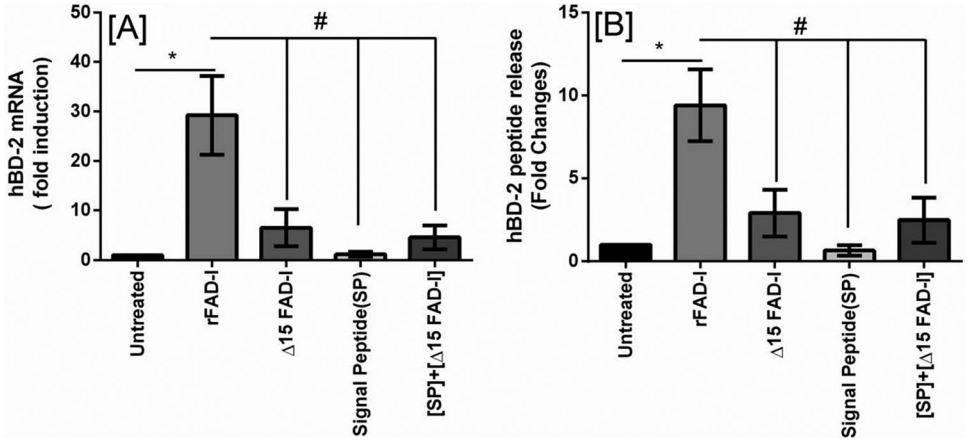

FIG 4 Comparison of hBD-2 induction and release from HOECs by rFAD-I, mature rFAD-I, and its signal peptide. HOECs were treated for 18 h with 10 μg/ml of the indicated peptides {rFAD-I, recombinant full-length FAD-I; Δ15 FAD-I, rFAD-I with the 15-amino-acid signal sequence deleted; Signal Peptide (SP), signal peptide only; [SP] + [Δ15 FAD-I], mixture of signal peptide and Δ15 FAD-I}. Fold changes in hBD-2 mRNA (A) and released peptide (B) compared to untreated HOECs were measured. The data presented are means ± SD of the results of six independent experiments; *, significant ($P < 0.05$) compared to untreated HOECs; #, significant ($P < 0.05$) compared to rFAD-I-treated cells.

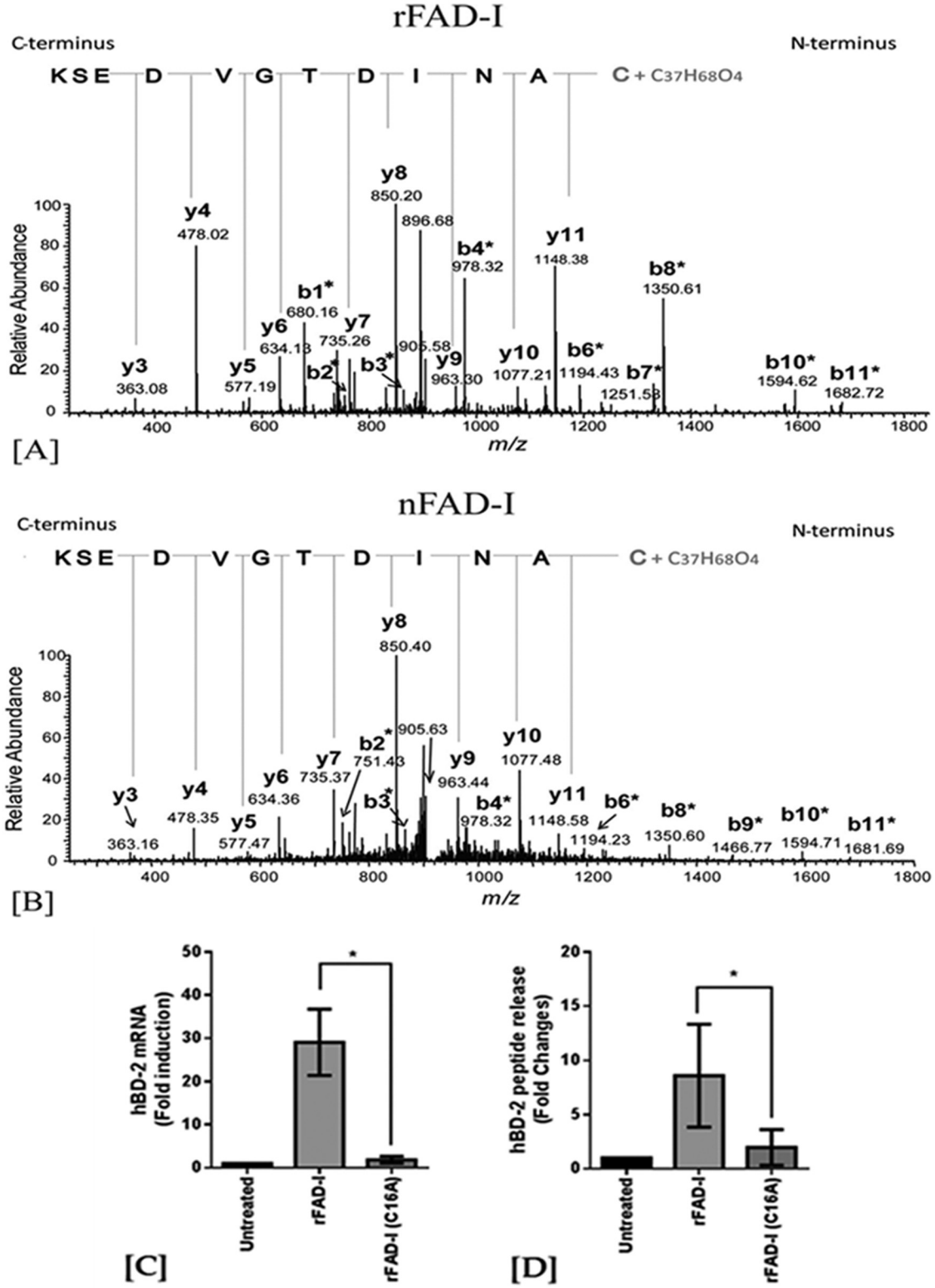

FIG 5 (A and B) Tandem-mass-spectrometry chromatograms for identification of the lipid moiety in rFAD-I (A) and nFAD-I (B). The chromatogram shows the doubly charged peptide CANIDTGVDESK at *m/z* 914.53, where Cys modified by 576.4 Da corresponds to *S*-diacylglycerol cysteine. The asterisk indicates modification. (C and D) HOECs were treated for 18 h with 10 μg/ml of each of the peptides, as indicated [rFAD-I, recombinant FAD-I; rFAD-I (C16A), rFAD-I with the cysteine at position 16 mutated to alanine]. Fold changes in hBD-2 mRNA (C) and released peptide (D) compared to untreated HOECs were determined. The data presented are means ± SD of the results of six independent experiments; *, $P < 0.05$.

protonated ion signals at *m/z* 914.53 derived from the FAD-I tryptic digest produced a spectrum in which all the observed b-fragment ions, including b1 to b11 ions, were shifted by +576.14 Da. In contrast, the observed y-fragment ions, including y1 to y11 ions, were unchanged. The shifting of the b1 to b11 ions but not the y1 to y11 ions by 576.4 Da is indicative of *S*-diacyl-glycerol modification at the cysteine residue of the CANIDTGVDESK peptide (i.e., the cysteine at position 16 of the full-length FAD-I peptide).

To investigate the importance of the lipidated C16 in hBD-2 induction, the cysteine was replaced by alanine (A) in rFAD-I. This significantly reduced the ability of FAD-I to induce hBD-2, indicating the importance of the cysteine-diacylglycerol modification in hBD-2 induction (Fig. 5C and D).

FAD-I-mediated hBD-2 induction is TLR-1/2 and TLR-2/6 dependent. Previously, we reported that the induction of hBD-2 by FAD-I is TLR-2 dependent (1). Here, we investigated if this TLR dependence included heterodimerization of TLR-2 with either TLR-1 or TLR-6. When we treated HOECs with FAD-I in the presence or absence of anti-TLR-1 or anti-TLR-6 antibody, we observed significantly diminished hBD-2 induction, indicating that TLR-2 interaction with both TLR-1 and TLR-6 is involved in induction of hBD-2 by FAD-I in HOECs (Fig. 6A).

To further investigate this observation, we conducted flow cytometric analysis to reveal the presence or absence of TLR receptors on HOEC surfaces after FAD-I challenge. Representative flow cytometric analysis demonstrated that both TLR-1/2 and TLR-2/6 are reduced on the surfaces of HOECs following FAD-I challenge, with more surface expression reduction of TLR-1 than of TLR-6 (Fig. 6B and D). Additionally, while both TLR-1 and TLR-6 were internalized in response to FAD-I, there was a greater percentage of TLR-1 internalization than of TLR-6 compared to untreated cells (Fig. 6B and C).

The FAD-I–TLR-2 interaction was additionally investigated using CytD, an inhibitor of actin polymerization, to see if blocking of receptor internalization can inhibit the reduction in TLR-2 surface expression in the presence of FAD-I. HOECs in the presence of CytD showed little change in TLR2 surface expression after challenge with FAD-I compared to FAD-I-treated HOECs alone (Fig. 6D). This was confirmed by using FITC-labeled rFAD-I in the presence and absence of CytD (Fig. 6E and F).

DISCUSSION

Previously, the cell wall of *F. nucleatum*, a ubiquitous bacterium of the oral cavity, was shown to induce hBD-2 in HOECs (5). More recently, using systematic biochemical fractionation of FnCW, we identified FAD-I as the hBD-2-inducing factor. This was further confirmed via functional heterologous expression of FAD-I in *P. gingivalis* (1). In our present study, we report differential induction of hBD-2 by different strains of *F. nucleatum*; ATCC 25586 and ATCC 23726 trigger significantly more hBD-2 mRNA production than ATCC 10953. ATCC 25586 and ATCC 23726 are therefore designated high inducers, while ATCC 10953 is designated a low inducer of hBD-2. Via heterologous expression of *fadI* from highly hBD-2-inducing strains in a Δ*fadI* derivative of the low-hBD-2-inducing strain ATCC 10953, we were able to restore FAD-I induction in the low inducer to levels comparable to those observed for the highly inducing strains.

In addition, by using antibodies specifically targeting FAD-I, we inhibited the high-inducer cell wall fraction from inducing hBD-2 by more than 80%. These two independent approaches support our contention that FAD-I is the principal cell wall-associated fusobacterial agent responsible for hBD-2 induction in HOECs.

Our mass spectroscopy analysis and replacement of cysteine (C16) with alanine revealed the importance of the posttranslational C16 diacylglycerol moiety in FAD-I in promoting hBD-2 expression in HOECs. Additionally, our *in silico* analysis revealed that all three *F. nucleatum* strains expressed a diacylglycerol moiety bound to cysteine in position 16. Therefore, that alone could not explain the strain-related differences in hBD-2 induction.

The Western immunoblot data using whole-cell lysates of *F. nucleatum* hBD2 low- and high-inducer strains showed reduced FAD-I expression in the whole-cell lysates of the low inducer (ATCC 10953) compared to the high inducers (ATCC 25586 and ATCC 23726), which was even more apparent when we used cell wall fractions for these strains (see Fig. S3 in the supplemental material). The mechanism of protein secretion in eukaryotes and prokaryotes requires the signal sequence to facilitate transport of the translated protein to the membrane (31), and it also helps the protein attain the right conformation required to maintain its functionality (32). The fact that the major sequence difference between the FAD-I of ATCC 10953 and those of the other two strains is in the signal peptide domain of FAD-I (Fig. 2; see Fig. S2 in the supplemental material) suggests that the variability in levels of FAD-I production and cell wall integration in ATCC 10953 compared to ATCC 25586 and ATCC 23726 could be due to variability in the efficiency of FAD-I signal peptide anchoring to the outer membranes of the respective strains. However, we cannot rule out the possibility that a conformational difference, as demonstrated by amino acid sequence differences in the mature-peptide region of FAD-I proteins from the hBD2 low- and high-inducer strains could also contribute to variability in hBD-2 induction in HOECs. The theoretically predicted structures of FAD-I proteins from ATCC 10953 and ATCC 25586 based on I-TASSER (iterative threading assembly refinement) (33, 34) showed differences in the residues predicted to interact with the TLRs (data not shown). Therefore, differences in FAD-I presentation from its cognate receptors, along with differences in levels of expression of FAD-I on the outer membranes of *F. nucleatum* strains, may collectively be responsible for variability in hBD-2 induction in HOECs. Deciphering this intriguing hypothesis will require additional work, which is under way in our laboratory.

Purified FAD-I proteins, resolved under denaturing conditions, resulted in two prominent bands, i.e., at 14 kDa and 12 kDa, as detected by Coomassie staining and Western blotting (see Fig. S4 in the supplemental material), indicating the presence of full-length and mature peptide in rFAD-I. Another *F. nucleatum* outer-membrane-associated protein, FadA, which has been shown to play an important role in binding and invasion of host cells by the organism, also exhibits a premature and a mature peptide when resolved by SDS-PAGE. The amino acid sequence analysis of FAD-I indicated the presence of a 15-amino-acid signal peptide. Challenging HOECs with recombinantly produced mature FAD-I, i.e., without the signal peptide (Δ15 FAD-I), significantly reduced its activity, and adding the signal peptide to the assay mixture in the presence of the mature peptide did not restore FAD-I activity to an appreciable extent. This suggests that the signal sequence and the mature peptide must be bound as a single unit to maintain conformational integrity for FAD-I activity when

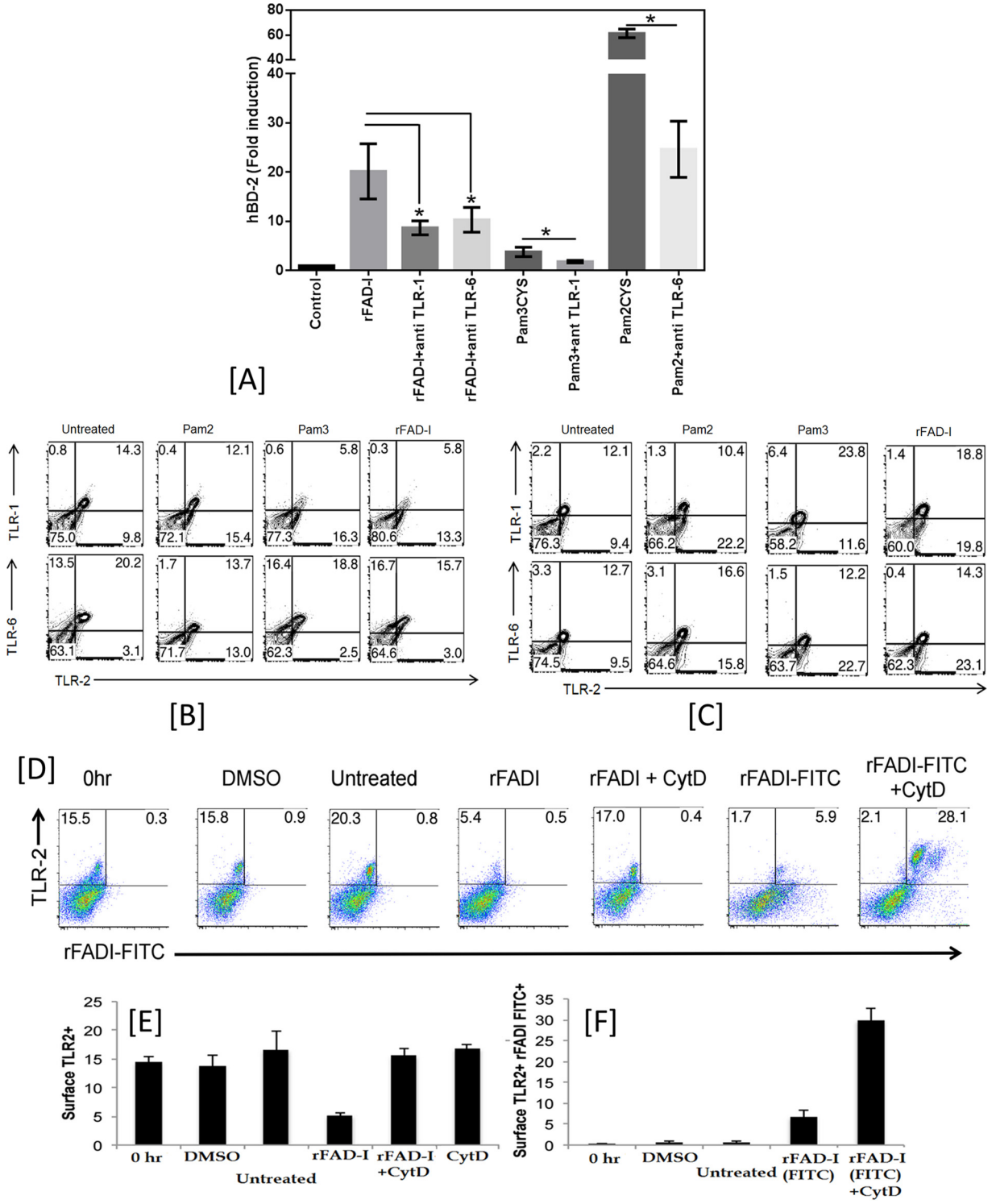

FIG 6 HOEC TLR-1/2 and TLR-2/6 interaction with rFAD-I. (A) HOECs were treated with either rFAD-I (10 μg/ml), Pam2Cys (a positive control for TLR-2/6; 20 ng/ml; Invivogen, USA), or Pam3Cys (a positive control for TLR-1/2; 20 ng/ml; Invivogen, USA) for 18 h in the presence or absence of anti-TLR antibodies (Invivogen, USA) as indicated. The antibodies were incubated with HOECs for 60 min prior to 18 h of incubation with the other reagents. HBD-2 mRNA fold changes compared to untreated HOECs were determined. The data presented are means ± SD of the results of three independent experiments; *, $P < 0.05$. (B and C) Flow cytometric analysis of TLR interaction with rFAD-I. HOECs were plated in 24-well clusters in duplicate. Upon attaining 70 to 80% confluence, the cells were harvested (0 h); left untreated (untreated); or incubated with either recombinant FAD-I (rFAD-I), Pam2Cys, or Pam3Cys for 30 min. Cells were harvested for surface staining (B) or intracellular detection (C) of TLRs by flow cytometry. (D to F) Flow cytometric analysis of TLR2 after rFAD-I and FITC-labeled rFAD-I challenge of cytochalasin D-treated HOECs. (D) Semiconfluent HOECs were harvested (0 h) and left untreated or treated with either dimethyl sulfoxide (DMSO), rFAD-I, rFAD-I plus CytD (Sigma, USA), FITC-labeled rFAD-I, or FITC-labeled rFAD-I plus CytD for 45 min. Cells were then harvested for TLR-2 surface staining and analyzed by flow cytometry. (E and F) The percentage of surface TLR2 (only)-expressing cells (E) or the percentage of surface $TLR2^+$ rFAD-I–FITC double-positive cells (F) among HOECs harvested at 0 h, incubated with DMSO (DMSO), left untreated (untreated), or incubated with FITC-labeled rFAD-I [rFAD-I (FITC)] for 30 min in the presence or absence of 40 μM CytD was determined. The flow cytometric data presented are representative of two independent experiments.

presented to HOECs as a standalone molecule. However, this may not be relevant *in vivo* when *F. nucleatum* comes in contact with HOECs, since the outer membrane, in which FAD-I would be embedded, would provide conformational stability to the molecule. According to Mascioni et al. (35), the amino terminus of bacterial lipoproteins may not only function to direct outer membrane localization, but also serve as an extended linker sequence, making the protein available at the extracellular surface.

Our current results show that nFAD-I and rFAD-I behave similarly in their ability to induce hBD-2. Mass spectrometric analysis demonstrated the presence of a PTM associated with the only cysteine in the molecule in both proteins. Interestingly, rFAD-I generated in *E. coli* retained the same posttranslational modification as nFAD-I, which we isolated from *F. nucleatum*, i.e., diacylglycerol and not triacylglycerol. The classical lipoprotein modification pathway in bacteria is composed of three sequential enzymatic reactions catalyzed by two acetyltransferases and one signal peptidase (36). The enzymes lipoprotein diacylglyceryl transferase (Lgt) and signal peptidase II (Lsp) are involved in producing diacylated lipoproteins (36), while triacylated lipoproteins are the result of additional catalysis steps by apolipoprotein *N*-acyltransferase (Lnt) (36, 37). We searched for these enzymes in the *F. nucleatum* ATTC 25586 genome database (38) and found Lgt (GeneID 991758; gene symbol, FN0489) and Lsp (GeneID 991403; gene symbol, FN0068) homologues, but not lnt, consistent with our finding that FAD-I is diacylated and not triacylated. Gram-negative bacteria are known to have lnt, which promotes triacylated-lipoprotein generation (39). *E. coli*, like other Gram-negative bacteria, expresses all three enzymes; however, in the generation of lipoproteins, lnt causes diacylated moieties to become triacylated, as it is the default enzyme that adds an acyl group to the N terminus of the diacylated molecule (36, 39). Thus, the lipid modification of FAD-I appears to be unique, as it is a diacyl peptide produced by a Gram-negative bacterium (*F. nucleatum*). It is also surprising that even when produced in *E. coli* it is diacylated, in spite of the presence of machinery for triacylation. We could speculate that there could be a specific recognition motif that determines the number of acyl groups added to the lipoprotein; however, while this opens up a new avenue for further investigation, it is beyond the scope of the present study.

The lipid moiety of a bacterial lipoprotein plays a crucial role in bacterium-host cell interactions. For example, lipidated peptides are discriminated by host TLRs on the basis of the degree of fatty acid acylation. Among the TLRs, TLR-2 plays a major role in the recognition of Gram-positive bacteria (40). Biochemical studies using cell wall component-deficient mutant bacteria demonstrated that bacterial lipoproteins, but not lipoteichoic acid or peptidoglycan, act as real native TLR-2 ligand molecules (41–43). Only the lipoproteins are real TLR-2 ligands, and the others may contain lipoproteins as contaminants during their preparation (44). In the present report, we show that FAD-I is a diacylated lipopeptide, and previously, we demonstrated that it induces hBD-2 in HOECs through TLR-2 (1). TLR-2 is unique in its ability to form heterodimer complexes with TLR-1 or TLR-6. Triacyl and diacyl synthetic lipopeptides, such as *N*-palmitoyl-*S*-dipalmitoylglyceryl CSK_4 and MALP-2, have been used as TLR-1/2 and TLR-2/6 agonists, respectively, leading to a model in which triacylated lipopeptides/lipoproteins activate through the TLR-1/2 heterodimer, whereas diacylated lipopeptides/lipoproteins activate through the TLR-2/6 heterodimer (45–47). Here, we report that induction of hBD-2 by diacylated FAD-I induces hBD-2 through both TLR-1/2 and TLR-2/6 in HOECs. Triacylated SitC lipoprotein purified from *Staphylococcus aureus* cells has been shown to stimulate immune cells via both TLR-1/2 and TLR-2/6 heterodimers (43), and some diacylated bacterial lipopeptides can also activate cells in a TLR-6-independent manner (48, 49).

In the context of induction of innate response elements in human oral mucosa, we envision that variability in hBD-2 induction could be the result of both the FAD-I expression level and conformation differences, as demonstrated by low- and high-inducer *F. nucleatum* strains, along with interpersonal variability in TLR levels of expression in oral mucosal cells (50).

Teleologically, bacterial molecules such as FAD-I, from various oral bacterial species, could be contributing to the regulation of homeostasis in the oral mucosa and thus explain why hBD-2, while inducible, is constitutively expressed in the oral mucosa with little concomitant inflammation. Interestingly, hBD-2 appears only in the presence of infection or inflammation in most tissues, including the skin (51), trachea (52), and gut epithelium (53, 54), sites where *F. nucleatum* is not a normal inhabitant. Furthermore, we have noticed that FAD-I does not induce interleukin 8 (IL-8) in HOECs (data not shown). Therefore, the interaction of FAD-I with the host mucosal epithelium, which results in expression of antimicrobials, such as hBD-2 (1) and CCL20 (10), without simultaneously triggering inflammatory mediator(s), may reflect an inherent strategy of symbiosis between certain bacteria and the host mucosa. The growing problem of resistance to conventional antibiotics and the need for new antimicrobials has stimulated interest in the development of antimicrobial peptides (AMPs), such as hBDs, as human therapeutics. Unlike conventional antibiotics, resistance by an organism to AMPs is surprisingly rare and difficult to generate (55–57). This is probably due to the nonspecific nature of the electrostatic/hydrophobic interaction of the AMP with various anionic components of the bacterial membrane (55, 56). We hypothesize that a new class of therapeutics could be developed that would facilitate the production of endogenous AMPs when needed and locally where applied. Identification and characterization of bacterial molecules, such as FAD-I, including understanding their interactions with the host, may one day offer a new paradigm in immunoregulatory therapeutics to promote mucosal protection at vulnerable body sites.

ACKNOWLEDGMENTS

This work was supported by NIH/NIDCR grants R01 DE018276 (A.W.) and RO1 DE021108 (R.L.).

We thank J. R. Blakemore, E. K. Schneider, W. S. Blood, S. Alperin, and F. Faddoul for providing normal human oral tissue.

A.W., T.S.M., R.L., and S.K.G. conceived the study. A.W., S.K.G, T.S.M., R.L., and P.P. analyzed and interpreted data. S.K.G. and A.W. wrote and prepared the manuscript. T.S.M. and R.L. edited the manuscript. S.B. purified nFAD-I and different mutants of rFAD-I and performed cell cultures, qPCR, ELISA, and Western immunoblotting. B.S. generated different mutants of *F. nucleatum*. S.N. and A.Y. developed the protocol and generated rFAD-I. J.K. performed mass spectrophotometric analysis of FAD-I. B.E. isolated primary human oral epithelial cells. P.P. performed flow cytometry for TLR internalization.

We declare that we have no conflicts of interest with the contents of this article.

FUNDING INFORMATION

This work, including the efforts of Aaron Weinberg, was funded by HHS | NIH | National Institute of Dental and Craniofacial Research (NIDCR) (R01 DE018276). This work, including the efforts of Renate Lux, was funded by HHS | NIH | National Institute of Dental and Craniofacial Research (NIDCR) (RO1 DE021108).

REFERENCES

1. **Gupta S, Ghosh SK, Scott ME, Bainbridge B, Jiang B, Lamont RJ, McCormick TS, Weinberg A.** 2010. Fusobacterium nucleatum-associated beta-defensin inducer (FAD-I): identification, isolation, and functional evaluation. J Biol Chem **285:**36523–36531. http://dx.doi.org/10.1074/jbc.M110.133140.
2. **Gomes PDS, Fernandes MH.** 2010. Defensins in the oral cavity: distribution and biological role. J Oral Pathol Med **39:**1–9. http://dx.doi.org/10.1111/j.1600-0714.2009.00832.x.
3. **Gursoy UK, Könönen E.** 2012. Understanding the roles of gingival beta-defensins. J Oral Microbiol **2012:**4. http://dx.doi.org/10.3402/jom.v4i0.15127.
4. **Hancock RE, Sahl HG.** 2006. Antimicrobial and host-defense peptides as new anti-infective therapeutic strategies. Nat Biotechnol **24:**1551–1557. http://dx.doi.org/10.1038/nbt1267.
5. **Krisanaprakornkit S, Kimball JR, Weinberg A, Darveau RP, Bainbridge BW, Dale BA.** 2000. Inducible expression of human beta-defensin 2 by Fusobacterium nucleatum in oral epithelial cells: multiple signaling pathways and role of commensal bacteria in innate immunity and the epithelial barrier. Infect Immun **68:**2907–2915. http://dx.doi.org/10.1128/IAI.68.5.2907-2915.2000.
6. **Dale BA, Krisanaprakornkit S.** 2001. Defensin antimicrobial peptides in the oral cavity. J Oral Pathol Med **30:**321–327. http://dx.doi.org/10.1034/j.1600-0714.2001.300601.x.
7. **Ji S, Shin JE, Kim YS, Oh JE, Min BM, Choi Y.** 2009. Toll-like receptor 2 and NALP2 mediate induction of human beta-defensins by fusobacterium nucleatum in gingival epithelial cells. Infect Immun **77:**1044–1052. http://dx.doi.org/10.1128/IAI.00449-08.
8. **Dommisch H, Reinartz M, Backhaus T, Deschner J, Chung W, Jepsen S.** 2012. Antimicrobial responses of primary gingival cells to Porphyromonas gingivalis. J Clin Periodontol **39:**913–922. http://dx.doi.org/10.1111/j.1600-051X.2012.01933.x.
9. **Ghosh SK, Gerken TA, Schneider KM, Feng Z, McCormick TS, Weinberg A.** 2007. Quantification of human beta-defensin-2 and -3 in body fluids: application for studies of innate immunity. Clin Chem **53:**757–765. http://dx.doi.org/10.1373/clinchem.2006.081430.
10. **Ghosh SK, Gupta S, Jiang B, Weinberg A.** 2011. Fusobacterium nucleatum and human beta-defensins modulate the release of antimicrobial chemokine CCL20/macrophage inflammatory protein 3α. Infect Immun **79:**4578–4587. http://dx.doi.org/10.1128/IAI.05586-11.
11. **Jin G, Kawsar HI, Hirsch SA, Zeng C, Jia X, Feng Z, Ghosh SK, Zheng QY, Zhou A, McIntyre TM, Weinberg A.** 2010. An antimicrobial peptide regulates tumor-associated macrophage trafficking via the chemokine receptor CCR2, a model for tumorigenesis. PLoS One **5:**e10993. http://dx.doi.org/10.1371/journal.pone.0010993.
12. **Kawsar HI, Weinberg A, Hirsch SA, Venizelos A, Howell S, Jiang B, Jin G.** 2009. Overexpression of human beta-defensin-3 in oral dysplasia: potential role in macrophage trafficking. Oral Oncol **45:**696–702. http://dx.doi.org/10.1016/j.oraloncology.2008.10.016.
13. **Doss M, White MR, Tecle T, Hartshorn KL.** 2010. Human defensins and LL-37 in mucosal immunity. J Leukoc Biol **87:**79–92. http://dx.doi.org/10.1189/jlb.0609382.
14. **Feng Z, Jia X, Adams MD, Ghosh SK, Bonomo RA, Weinberg A.** 2014. Epithelial innate immune response to Acinetobacter baumannii challenge. Infect Immun **82:**4458–4465. http://dx.doi.org/10.1128/IAI.01897-14.
15. **Ganz T.** 2003. Defensins: antimicrobial peptides of innate immunity. Nat Rev Immunol **3:**710–720. http://dx.doi.org/10.1038/nri1180.
16. **Kimball JR, Nittayananta W, Klausner M, Chung WO, Dale BA.** 2006. Antimicrobial barrier of an in vitro oral epithelial model. Arch Oral Biol **51:**775–783. http://dx.doi.org/10.1016/j.archoralbio.2006.05.007.
17. **Yin L, Dale BA.** 2007. Activation of protective responses in oral epithelial cells by Fusobacterium nucleatum and human beta-defensin-2. J Med Microbiol **56:**976–987. http://dx.doi.org/10.1099/jmm.0.47198-0.
18. **Pazgier M, Prahl A, Hoover DM, Lubkowski J.** 2007. Studies of the biological properties of human beta-defensin 1. J Biol Chem **282:**1819–1829. http://dx.doi.org/10.1074/jbc.M607210200.
19. **Harder J, Gläser R, Schröder JM.** 2007. Human antimicrobial proteins: effectors of innate immunity. J Endotoxin Res **13:**317–338. http://dx.doi.org/10.1177/0968051907088275.
20. **Weinberg A, Jin G, Sieg S, McCormick TS.** 2012. The yin and yang of human beta-defensins in health and disease. Front Immunol **3:**294. http://dx.doi.org/10.3389/fimmu.2012.00294.
21. **Kolenbrander PE, Palmer RJ, Jr, Periasamy S, Jakubovics NS.** 2010. Oral multispecies biofilm development and the key role of cell-cell distance. Nat Rev Microbiol **8:**471–480. http://dx.doi.org/10.1038/nrmicro2381.
22. **Kolenbrander PE.** 2011. Multispecies communities: interspecies interactions influence growth on saliva as sole nutritional source. Int J Oral Sci **3:**49–54. http://dx.doi.org/10.4248/IJOS11025.
23. **Krisanaprakornkit S, Kimball JR, Dale BA.** 2002. Regulation of human beta-defensin-2 in gingival epithelial cells: the involvement of mitogen-activated protein kinase pathways, but not the NF-kappaB transcription factor family. J Immunol **168:**316–324. http://dx.doi.org/10.4049/jimmunol.168.1.316.
24. **Oda D, Watson E.** 1990. Human oral epithelial cell culture. I. Improved conditions for reproducible culture in serum-free medium. In Vitro Cell Dev Biol **26:**589–595.
25. **Haake SK, Yoder SC, Attarian G, Podkaminer K.** 2000. Native plasmids of Fusobacterium nucleatum: characterization and use in development of genetic systems. J Bacteriol **182:**1176–1180. http://dx.doi.org/10.1128/JB.182.4.1176-1180.2000.
26. **Shevchuk NA, Bryksin AV, Nusinovich YA, Cabello FC, Sutherland M, Ladisch S.** 2004. Construction of long DNA molecules using long PCR-based fusion of several fragments simultaneously. Nucleic Acids Res **32:**e19. http://dx.doi.org/10.1093/nar/gnh014.
27. **Kaplan A, Kaplan CW, He X, McHardy IH, Shi W, Lux R.** 2014. Characterization of *aid1*, a novel gene involved in *Fusobacterium nucleatum* interspecies interactions. Microb Ecol **68:**379–387. http://dx.doi.org/10.1007/s00248-014-0400-y.
28. **Kennell W, Holt SC.** 1990. Comparative studies of the outer membranes of Bacteroides gingivalis, strains ATCC 33277, W50, W83, 381. Oral Microbiol Immunol **5:**121–130. http://dx.doi.org/10.1111/j.1399-302X.1990.tb00409.x.
29. **Rozen S, Skaletsky H.** 2000. Primer3 on the WWW for general users and for biologist programmers. Methods Mol Biol **132:**365–386.
30. **de Castro E, Sigrist CJ, Gattiker A, Bulliard V, Langendijk-Genevaux PS, Gasteiger E, Bairoch A, Hulo N.** 2006. ScanProsite: detection of PROSITE signature matches and ProRule-associated functional and structural residues in proteins. Nucleic Acids Res **34:**W362–W365. http://dx.doi.org/10.1093/nar/gkl124.
31. **Emr SD, Silhavy TJ.** 1983. Importance of secondary structure in the signal sequence for protein secretion. Proc Natl Acad Sci U S A **80:**4599–4603. http://dx.doi.org/10.1073/pnas.80.15.4599.
32. **Singh P, Sharma L, Kulothungan SR, Adkar BV, Prajapati RS, Ali PS, Krishnan B, Varadarajan R.** 2013. Effect of signal peptide on stability and folding of Escherichia coli thioredoxin. PLoS One **8:**e63442. http://dx.doi.org/10.1371/journal.pone.0063442.
33. **Roy A, Kucukural A, Zhang Y.** 2010. I-TASSER: a unified platform for automated protein structure and function prediction. Nat Protoc **5:**725–738. http://dx.doi.org/10.1038/nprot.2010.5.
34. **Zhang Y.** 2008. I-TASSER server for protein 3D structure prediction. BMC Bioinformatics **9:**40. http://dx.doi.org/10.1186/1471-2105-9-40.
35. **Mascioni A, Bentley BE, Camarda R, Dilts DA, Fink P, Gusarova V, Hoiseth SK, Jacob J, Lin SL, Malakian K, McNeil LK, Mininni T, Moy F, Murphy E, Novikova E, Sigethy S, Wen Y, Zlotnick GW, Tsao DH.** 2009. Structural basis for the immunogenic properties of the meningococcal vaccine candidate LP2086. J Biol Chem **284:**8738–8746. http://dx.doi.org/10.1074/jbc.M808831200.
36. **Kovacs-Simon A, Titball RW, Michell SL.** 2011. Lipoproteins of bacterial pathogens. Infect Immun **79:**548–561. http://dx.doi.org/10.1128/IAI.00682-10.
37. **Tokuda H.** 2009. Biogenesis of outer membranes in Gram-negative bacteria. Biosci Biotechnol Biochem **73:**465–473. http://dx.doi.org/10.1271/bbb.80778.
38. **Kapatral V, Anderson I, Ivanova N, Reznik G, Los T, Lykidis A, Bhattacharyya A, Bartman A, Gardner W, Grechkin G, Zhu L, Vasieva O, Chu L, Kogan Y, Chaga O, Goltsman E, Bernal A, Larsen N, D'Souza**

M, Walunas T, Pusch G, Haselkorn R, Fonstein M, Kyrpides N, Overbeek R. 2002. Genome sequence and analysis of the oral bacterium Fusobacterium nucleatum strain ATCC 25586. J Bacteriol **184:**2005–2018. http://dx.doi.org/10.1128/JB.184.7.2005-2018.2002.

39. **Tschumi A, Nai C, Auchli Y, Hunziker P, Gehrig P, Keller P, Grau T, Sander P.** 2009. Identification of apolipoprotein N-acyltransferase (Lnt) in mycobacteria. J Biol Chem **284:**27146–27156. http://dx.doi.org/10.1074/jbc.M109.022715.
40. **Takeuchi O, Hoshino K, Kawai T, Sanjo H, Takada H, Ogawa T, Takeda K, Akira S.** 1999. Differential roles of TLR2 and TLR4 in recognition of gram-negative and gram-positive bacterial cell wall components. Immunity **11:**443–451. http://dx.doi.org/10.1016/S1074-7613(00)80119-3.
41. **Hashimoto M, Tawaratsumida K, Kariya H, Aoyama K, Tamura T, Suda Y.** 2006. Lipoprotein is a predominant Toll-like receptor 2 ligand in Staphylococcus aureus cell wall components. Int Immunol **18:**355–362.
42. **Hashimoto M, Tawaratsumida K, Kariya H, Kiyohara A, Suda Y, Krikae F, Kirikae T, Götz F.** 2006. Not lipoteichoic acid but lipoproteins appear to be the dominant immunobiologically active compounds in Staphylococcus aureus. J Immunol **177:**3162–3169. http://dx.doi.org/10.4049/jimmunol.177.5.3162.
43. **Kurokawa K, Lee H, Roh KB, Asanuma M, Kim YS, Nakayama H, Shiratsuchi A, Choi Y, Takeuchi O, Kang HJ, Dohmae N, Nakanishi Y, Akira S, Sekimizu K, Lee BL.** 2009. The triacylated ATP binding cluster transporter substrate-binding lipoprotein of Staphylococcus aureus functions as a native ligand for Toll-like receptor 2. J Biol Chem **284:**8406–8411. http://dx.doi.org/10.1074/jbc.M809618200.
44. **Nakayama H, Kurokawa K, Lee BL.** 2012. Lipoproteins in bacteria: structures and biosynthetic pathways. FEBS J **279:**4247–4268. http://dx.doi.org/10.1111/febs.12041.
45. **Takeda K, Takeuchi O, Akira S.** 2002. Recognition of lipopeptides by Toll-like receptors. J Endotoxin Res **8:**459–463. http://dx.doi.org/10.1177/09680519020080060101.
46. **Takeuchi O, Akira S.** 2010. Pattern recognition receptors and inflammation. Cell **140:**805–820. http://dx.doi.org/10.1016/j.cell.2010.01.022.
47. **Takeuchi O, Kawai T, Mühlradt PF, Morr M, Radolf JD, Zychlinsky A, Takeda K, Akira S.** 2001. Discrimination of bacterial lipoproteins by Toll-like receptor 6. Int Immunol **13:**933–940. http://dx.doi.org/10.1093/intimm/13.7.933.
48. **Buwitt-Beckmann U, Heine H, Wiesmüller KH, Jung G, Brock R, Akira S, Ulmer AJ.** 2005. Toll-like receptor 6-independent signaling by diacylated lipopeptides. Eur J Immunol **35:**282–289. http://dx.doi.org/10.1002/eji.200424955.
49. **Buwitt-Beckmann U, Heine H, Wiesmüller KH, Jung G, Brock R, Akira S, Ulmer AJ.** 2006. TLR1- and TLR6-independent recognition of bacterial lipopeptides. J Biol Chem **281:**9049–9057. http://dx.doi.org/10.1074/jbc.M512525200.
50. **Kinane DF, Shiba H, Stathopoulou PG, Zhao H, Lappin DF, Singh A, Eskan MA, Beckers S, Waigel S, Alpert B, Knudsen TB.** 2006. Gingival epithelial cells heterozygous for Toll-like receptor. Genes Immun **7:**190–200. http://dx.doi.org/10.1038/sj.gene.6364282.
51. **Ong PY, Ohtake T, Brandt C, Strickland I, Boguniewicz M, Ganz T, Gallo RL, Leung DY.** 2002. Endogenous antimicrobial peptides and skin infections in atopic dermatitis. N Engl J Med **347:**1151–1160. http://dx.doi.org/10.1056/NEJMoa021481.
52. **Starner TD, Agerberth B, Gudmundsson GH, McCray PB, Jr.** 2005. Expression and activity of beta-defensins and LL-37 in the developing human lung. J Immunol **174:**1608–1615. http://dx.doi.org/10.4049/jimmunol.174.3.1608.
53. **O'Neil DA, Porter EM, Elewaut D, Anderson GM, Eckmann L, Ganz T, Kagnoff MF.** 1999. Expression and regulation of the human beta-defensins hBD-1 and hBD-2 in intestinal epithelium. J Immunol **163:**6718–6724.
54. **Wehkamp J, Fellermann K, Herrlinger KR, Baxmann S, Schmidt K, Schwind B, Duchrow M, Wohlschläger C, Feller AC, Stange EF.** 2002. Human beta-defensin 2 but not beta-defensin 1 is expressed preferentially in colonic mucosa of inflammatory bowel disease. Eur J Gastroenterol Hepatol **14:**745–752. http://dx.doi.org/10.1097/00042737-200207000-00006.
55. **Diamond G, Beckloff N, Weinberg A, Kisich KO.** 2009. The roles of antimicrobial peptides in innate host defense. Curr Pharm Des **15:**2377–2392. http://dx.doi.org/10.2174/138161209788682325.
56. **Zasloff M.** 2002. Antimicrobial peptides of multicellular organisms. Nature **415:**389–395. http://dx.doi.org/10.1038/415389a.
57. **Ge Y, MacDonald DL, Holroyd KJ, Thornsberry C, Wexler H, Zasloff M.** 1999. In vitro antibacterial properties of pexiganan, an analog of magainin. Antimicrob Agents Chemother **43:**782–788.
58. **Larkin MA, Blackshields G, Brown NP, Chenna R, McGettigan PA, McWilliam H, Valentin F, Wallace IM, Wilm A, Lopez R, Thompson JD, Gibson TJ, Higgins DG.** 2007. Clustal W and Clustal X version 2.0. Bioinformatics **23:**2947–2948. http://dx.doi.org/10.1093/bioinformatics/btm404.